

MONITORING OF FATIGUE IN COMPOSITES USING AIR-COUPLED GUIDED WAVES

**Martin RHEINFURTH, Daniel DÖRING, Florian GEHRIG*, Igor SOLODOV,
Karl SCHULTE*, and Gerd BUSSE**

INSTITUTE OF POLYMER-TECHNOLOGY, DEPARTMENT OF NON-DESTRUCTIVE
TESTING (IKT-ZFP), UNIVERSITY OF STUTTGART,
32 Pfaffenwaldring, Stuttgart 70569, Germany

* INSTITUTE OF POLYMERS AND COMPOSITES, HAMBURG UNIVERSITY OF
TECHNOLOGY
5 Nesspriel, Hamburg 21129, Germany

Abstract

The objective of this paper is to develop a non-destructive methodology for remote monitoring of fatigue induced by mechanical load in fibre reinforced plastics. The approach is based on mode conversion of air-coupled ultrasound to flexural waves. Variations in flexural wave velocity and attenuation are used as indicators of fatigue state. Glass fibre reinforced non-crimp fabric plastic specimens were stepwise fatigued and measured in a single sided access configuration. The experiments conducted demonstrate that accumulated fatigue is accompanied by decrease in velocity and increase in attenuation of the flexural wave. The change in wave velocity throughout fatigue is shown to correlate closely with measurements of stiffness degradation of the composite. This parameter is found to be different for different fatigue loading protocols. The propagation of flexural waves is affected by internal interfaces such as cracks due to scattering. Hence, attenuation can be used as a measure of an increase in crack density caused by fatigue. The combination of wave velocity and attenuation is considered to be a distinctive parameter, which enables to determine whether the composite is fatigued in tension-tension or compression-tension mode.

Introduction

The volume of fibre reinforced plastics (FRP) in various applications (aircraft industry, wind energy engineering, etc) has been rising enormously for the last decade. The performance of FRP components is affected by structural degradation resulting from many factors, like environmental conditions, manufacturing defects, damage due to impact or/and fatigue. Fatigue damage is particularly important in high-risk applications where the components encounter many load cycles during their lifetime. Cyclic loading may lead to internal accumulation of damage in the composite resulting in a reduced residual strength [1] and eventually in a catastrophic failure. The non-destructive detection of fatigue induced defects, which degrade the structural integrity, is pursued to reduce the disadvantage of the complicated failure mechanism of FRP compared to metals. Innovative methodologies are needed to monitor composite degradation in operation to guarantee functionality and avoid unnecessary replacement of components.

Several techniques (acoustic emission, electric resistivity, optical fibres etc.) have been proposed for detection and characterization of fatigue damage in FRP caused by cyclic loading. Each of the techniques comes along with its drawbacks such as expensive sensors for structural health monitoring using smart structures or challenging application in industrial envi-

ronment. One of the approaches is based on the correlation between fatigue damage and stiffness change of composite structures. It has been reported [1–3] that FRP exhibits stiffness degradation in direction of loading accompanied by an increasing crack density. These features provide useful information on the structural integrity of composites. However, both stiffness and crack density are difficult to determine in industrial environment.

Conventional ultrasonic technique for probing material stiffness involves direct measurements of bulk wave velocities. For plate-like composite components the major loading direction is in-plane. However, ultrasonic testing of the in-plane stiffness is impeded by the availability of a single propagation direction across the thickness of the specimen [4]. For out-of-plane stiffness, the correlation between fatigue and velocity/attenuation has been measured in transmission mode [5]. This configuration does not provide single-sided access and has not been proven to be used in-situ. Furthermore, the data obtained in transmission mode are often not applicable to fatigue monitoring in strongly heterogeneous composite materials.

Ultrasonic Lamb (guided or plate) waves offer a convenient method for recovering in-plane elastic properties [6, 7]. The contact Lamb wave setups were found to be applicable to monitoring fatigue and thermal damage [8-10]. It was shown that the guided wave attenuation is sensitive to cracking induced by fatigue for a circumferential wave propagating in a hollow FRP cylinder [11].

Air-coupled ultrasound (ACU) has been increasingly used for inspection of plate-like components in recent years due to its advantage of being a non-contact and no-immersion methodology [12]. The conventional normal transmission mode has been modified to provide mode conversion of air-coupled ultrasound to Lamb waves for remote non-destructive evaluation in a single-sided access configuration [13]. A similar technique was recently applied to measuring phase velocity and attenuation for testing the moisture content and the micro cracking in carbon fibre reinforced plastic [14].

In this paper, the ACU mode conversion is applied to the study of wave velocity and attenuation in cyclic loaded non-crimp fibre (NCF) composite. It is shown that these parameters correlate with stiffness degradation and crack density. That enables to use this technique for monitoring of fatigue in NCF induced by mechanical loads.

Specimen Preparation and Fatigue Loading Protocol

A quadraxial NCF made of glass fibres was infiltrated with an epoxy resin. The composite was manufactured by a resin transfer moulding process to 2mm thick plates. The NCF consists of eight layers ($0^\circ/45^\circ/90^\circ/-45^\circ/45^\circ/90^\circ/-45^\circ/0^\circ$). The plies contain different amount of fibres (49% in 0° , 23% in 45° , 23% in -45° and 5% in 90°). A part of the virgin composite plate can be seen in the light transmission image in Fig. 2. The fibres are not visible but the binding yarn of the fabric is shown.

The produced plates were reinforced with FRP/aluminium edge flanges for loading grips and cut by a diamond blade into dimensions of 250mm in length and 25 or 50mm width. The fatigue tests were performed on servo hydraulic actuators using a frequency of $f=6\text{Hz}$ for cyclic loading. The stress ratio R is defined as the relation between the minimum and the maximum stress during one cycle. That means that $R=0.1$ is in the tensile regime and $R=-1$ contains tensile and compressive loads in one cycle. The Young's modulus in load direction was calcu-

lated from the geometry of the specimens and the strain measured by the servo hydraulic actuators.

The typical patterns of stiffness degradation and increase in crack density throughout a fatigue cycle are shown in Fig. 1 and clearly represent three phases of fatigue state in a FRP. In the first test trial, five narrow (25 mm wide) specimens were loaded at a stress ratio of $R=0.1$ at a maximum stress of $\sigma_{max}= 360$ MPa. For each specimen, the ACU measurements were made before the load application and successively after 50, 300, 1000 and 3500 cycles. Due to a premature failure of flanges occurred during loading test, the measurements were interrupted in the second phase of fatigue.

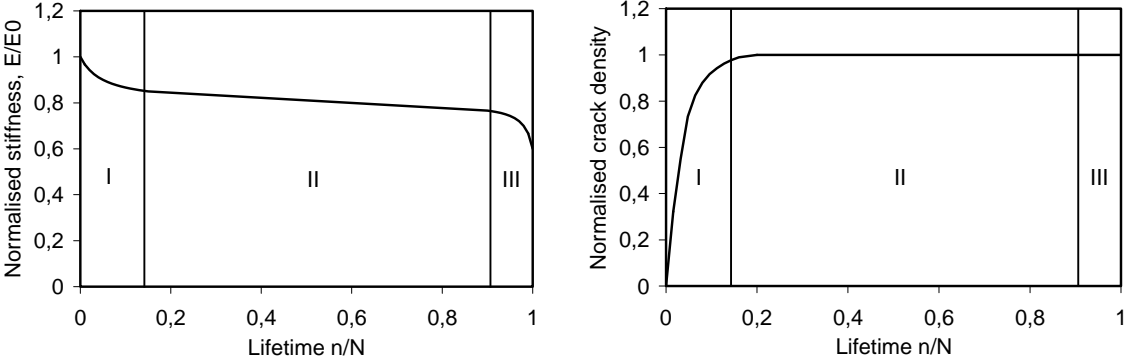


Fig. 1: Evolution of stiffness (left) and crack density (right) in composites during fatigue.

In the second test, the wider specimens (50 mm) were fatigued at different load levels in $R=0.1$ and $R=-1$ modes into the second phase of fatigue to provide a homogeneous crack distribution in the material. The ACU measurements were conducted only before and after cyclic loading. The crack pattern for a specimen fatigued at $R=0.1$ is shown in Fig. 2. The cracks were formed in the $\pm 45^\circ$ and 90° layers accompanied by edge delaminations (planar cracks parallel to the surface). The cracks in different oriented layers influence each other and create further delaminations.

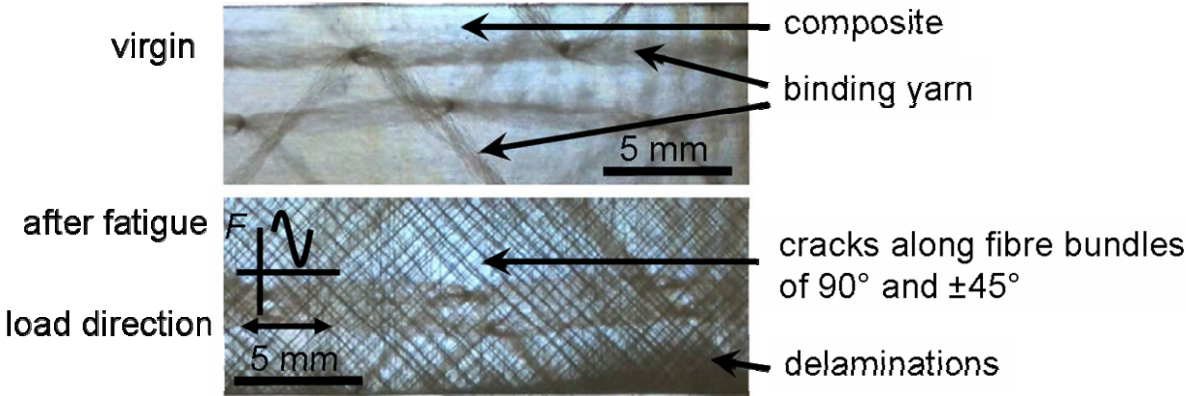


Fig. 2: Light transmission image of the intact (top) and the specimen after fatigue in $R=0.1$ cyclic mode (bottom).

In $R=-1$ cyclic mode the crack pattern developed similarly (Fig. 3); some additional cracks along the load bearing fibres (0° direction) also occurred.

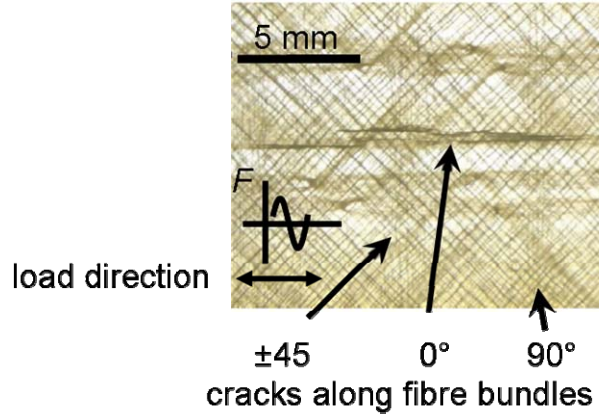


Fig. 3: Transmission image of the crack pattern after fatigue in R=-1 cyclic mode.

Experimental Methodology

The mode conversion of ACU is based on resonance excitation of plate (Lamb) waves in oblique incidence if the angle θ satisfies the relation [15]:

$$\sin \theta = V_a / V_p, \quad (1)$$

where V_a is the phase velocity of ultrasound in air and V_p is the phase velocity of the plate wave mode. This relation also defines the angles of the re-radiation of ultrasound in air from both sides of the specimen by the propagating wave. In particular, it enables to use a single sided configuration (Fig. 4) where the values of θ correspond to the maximum output signal obtainable by varying the angular positions of the transducers.

The efficiency of excitation/reception also depends on the plate wave mode; the maximum coupling between ACU and plate wave is provided for the zero-order antisymmetric mode (a_0) with predominately out-of-plane polarization [16]. In the experiments, commercial 200kHz air-coupled transducers with a circular aperture of 8mm diameter were used. For small values of θ (10^0 - 15^0), the size of excitation area was of the order of only (1-2) wavelengths for the a_0 -mode, so that excitation/reception was observed within a certain range of angles of incidence ($\sim 5^\circ$). That enabled to use the same settings for a variety of specimens of slightly different thickness and stiffness, which makes the method applicable *in-situ*.

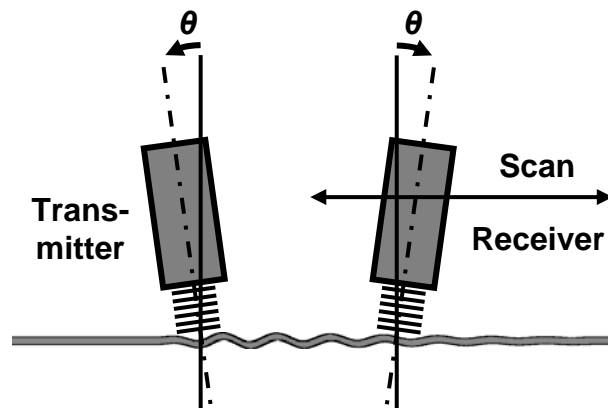


Fig. 4: Single-sided air-coupled configuration.

To measure the plate wave velocity and attenuation, the receiver is moved stepwise along the propagation path of the wave [17]. The Discrete Fourier Transformation (DFT) of the output signal is used to obtain the amplitude and phase at each step, which needs to be rather small. These values as functions of the distance between the transducers are used to calculate the plate wave velocity and attenuation.

The major contribution to the attenuation comes from damping (scattering and viscoelastic effects) and diffraction losses due to a finite aperture of the plate wave beam. To find out the impact of the diffraction, a C-scan of the wave field generated was carried out by moving only the receiving transducer. The result (Fig. 5) shows that the beam divergence is rather small for the propagation distance (x) in the far field zone ($>(10-15)$ mm). Such behaviour indicates the “self-focussing” effect for the plate wave in the NCF composite. The bundles or group of bundles of fibres (Fig. 2) act as a waveguide focussing the wave field and thus supporting a quasi-plane wave propagation. This effect reduces but does not exclude completely the diffraction losses in the NCF. The amplitude variation of a quasi-plane plate wave can therefore be approximated by an exponential decay:

$$A(x) = A_0 e^{-\alpha x}, \quad (2)$$

where α is the factor of attenuation caused by viscoelasticity and scattering. Two examples of attenuation measurements in a NCF specimen before and after cyclic loading are shown in Fig. 6. Some discrepancy between the measurement data and the exponential fit is obviously seen; however, averaging of a few measurements over the width of each specimen has been proven to lead to reasonable results.

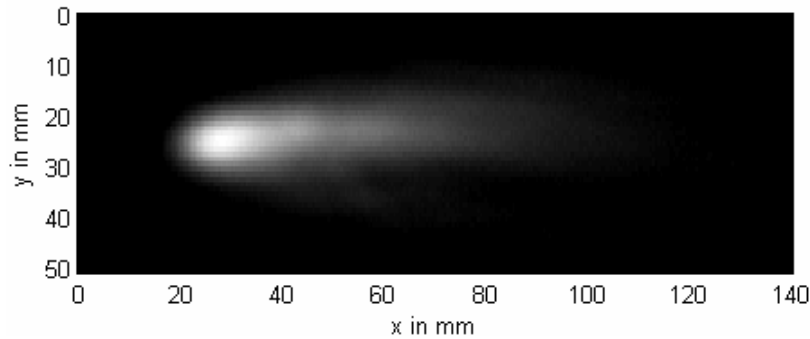


Fig. 5: C-scan image of the plate wave field in a 50mm wide NCF composite plate.

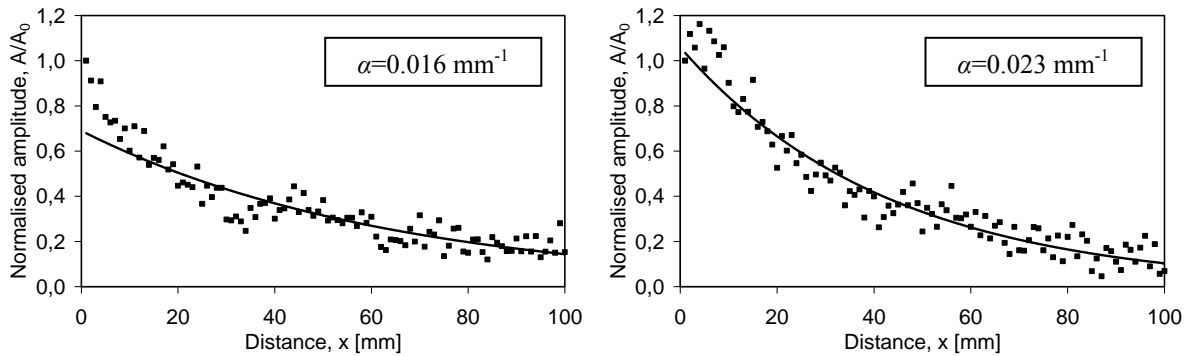


Fig. 6: Measurements of plate wave attenuation in NCF specimen before (left) and after (right) cyclic loading.

The plate wave velocity and attenuation measured along the axis of the cyclic load were then used for the evaluation of fatigue state. Precise alignment of the receiver path parallel to the specimen surface is crucial for measuring the plate wave velocity. For the specimens investigated, a deviation from parallelism of 0.1 degrees leads to an inaccuracy of 0.5% in plate wave velocity.

The relation between velocity of the a_0 -mode (V_{a0}) and the material stiffness can be obtained from the following equation [15]:

$$V_{a0} \approx \sqrt[4]{\frac{E}{3\rho(1-\nu^2)}} \sqrt{\pi \cdot f \cdot d}, \quad (3)$$

where E is the Young's modulus, ρ is the density, ν is the Poisson's ratio, f is the frequency and d is the thickness of the plate. Equation (3) is derived for waves in isotropic plates considered acoustically thin (flexural wave), however, it can also be applied for waves in symmetry directions of anisotropic materials [18]. Based on this approximation, the variation in material stiffness (Young's modulus) can be evaluated (assuming $1-\nu^2 \approx 1$) from the measurements of flexural wave velocities

$$\frac{E_0}{E_f} \approx \left(\frac{V_{a00}}{V_{a0f}} \right)^4, \quad (4)$$

where the indices 0 and f refer to intact and fatigued specimens, respectively.

Results

The stiffness degradation and variation in flexural wave velocity caused by cyclic loading were measured for the first group of 5 stepwise fatigued specimens. For the second group of specimens (11 samples with a different fatigue state each), the measurements were complemented by variation in attenuation for different cyclic loading modes.

For the stepwise fatigued specimens, the velocity of the flexural wave decreases rapidly within the first few hundred cycles, as shown in Fig. 7. This corresponds to the first phase of fatigue life, which can be characterised by exponential decline in stiffness, as illustrated in Fig. 1 (left). The second phase of composite fatigue accompanied by moderate stiffness degradation (Fig. 1) corresponds to a gradual decline in the wave velocity (Fig. 7). Inaccurate alignment of the specimens is assumed to result in the rise of the velocity after 1000 load cycles for specimen 2 and 3 in Fig. 7.

The experimental data for the stiffness variation through cyclic loading are illustrated in Fig. 8 for specimen 5. As expected, the stiffness measured by the servo hydraulic machine gradually decreases; the interruptions at 300 and 1000 cycles are caused by the changes of clamping after the specimens were removed from the testing machine for the ACU wave velocity measurements. The lower curve in Fig. 8 shows the variation in stiffness calculated from the wave velocity measurements based on Equation 4. A reasonable agreement between the two curves illustrates the applicability of the approach used for evaluation of fatigue induced stiffness degradation from the velocity measurements.

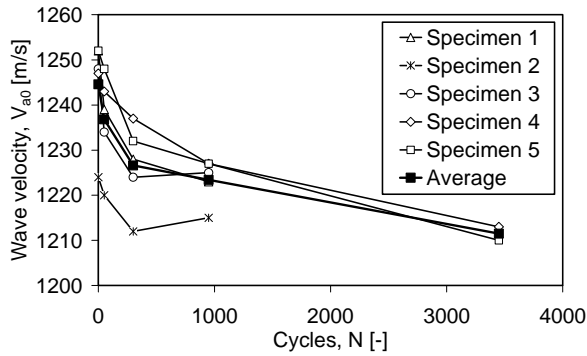


Fig. 7: Flexural wave velocities as functions of number of cycles in phase I/II of fatigue.

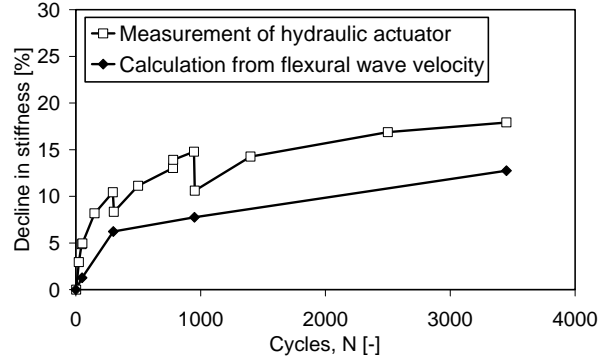


Fig. 8: Relative stiffness degradation and flexural wave velocity decline over number of cycles (specimen 5).

The experimental data on the second group of 11 specimens are presented in Figs. 9-12. All the specimens manifest 20-25% relative decline in stiffness (Fig. 9), which is basically independent of the number of cycles. The stiffness degradation for the two cyclic modes (tension-tension and compression-tension) is also virtually identical. That confirms a similarity in the fatigue state (phase II) of all the specimens.

The measurements of the attenuation reveal an increase in dissipation in phase II of fatigue (Fig. 10). Since the crack density stays constant in this phase (Fig. 1, right), the attenuation due to scattering is not expected to vary either. Unfortunately, the variability of the data in Fig. 10 is too large to make a tangible conclusion on the attenuation behaviour throughout phase II of fatigue. For this purpose further experiments, which relate closely to the fatigue history of each specimen, are in development.

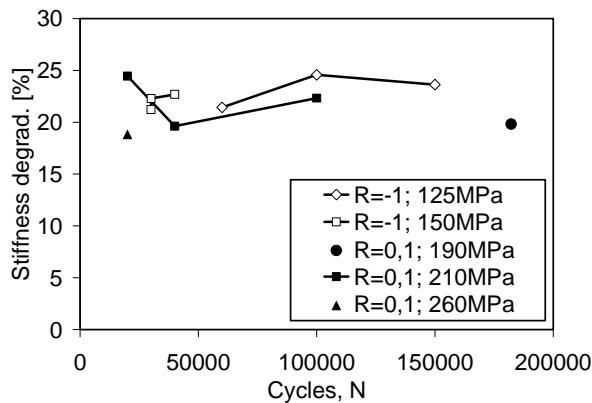


Fig. 9: Relative stiffness degradation caused by various modes of cyclic loading (phase II of fatigue).

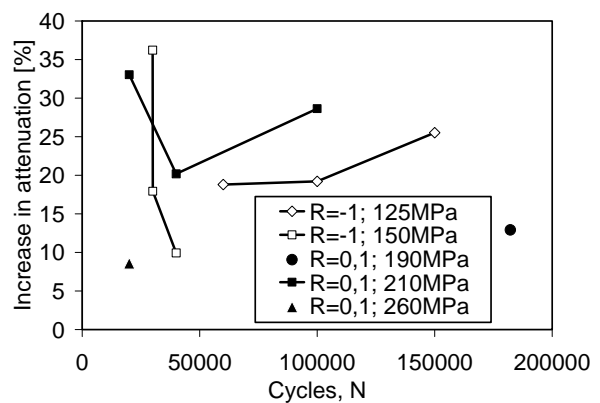


Fig.10: Relative increase in flexural wave attenuation due to cyclic loading (phase II of fatigue).

As mentioned above, the measurements of Young's modulus in the loading direction (Fig. 9) indicate no difference between the fatigue damage induced in tension-tension and compression-tension cyclic modes. This difference, however, is noticeable in Fig. 11, where the data on velocity variation are plotted as a function of the stiffness degradation. The tension-tension results in the lower velocity variation than that for the compression-tension cyclic mode in the same range of stiffness variation.

Since the information on in-plane degradation is difficult to retrieve in-situ, an alternative approach can use the measurements of the flexural wave attenuation in combination with the

velocity. The data on increase in velocity are plotted as a function of the attenuation variation (Fig. 12), which enables to distinguish between the fatigue caused by different cyclic modes in-situ.

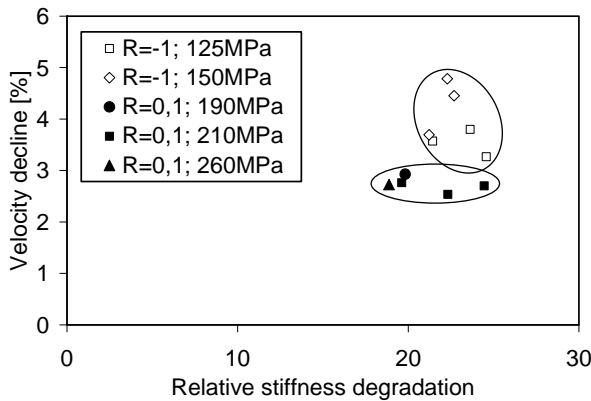


Fig. 11: Relative decline in flexural wave velocity as a function of stiffness degradation.

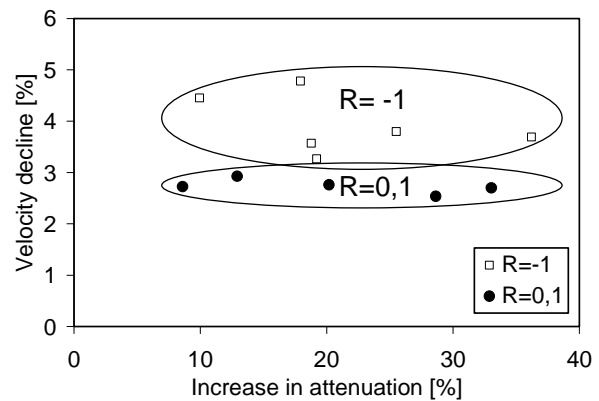


Fig. 12: Relation between variation in velocity and attenuation for flexural waves in NCF composite.

Discussion

The relation between the stiffness degradation and the flexural wave velocity for NCF composite fatigued in tension-tension and compression-tension modes suggests further considerations. The results show that a difference in flexural wave velocity is observed even when no substantial variation in overall Young's modulus in direction of the load is measured (Fig. 11). Generally, two major reasons for that can be indicated as discussed below.

The strain distribution in a plate caused by plate waves is a function of depth, so that the distinctive stiffness in each ply is relevant for the wave velocity. On the contrary, the stiffness measured in the servo hydraulic machine is averaged over the thickness of the specimen. For the NCF composite specimens studied, the maximum contribution to the bending stiffness, which is crucial for the flexural wave velocity, is expected by the surface plies while the role of the inner plies is diminished. Hence, the velocity measurements in the specimens fatigued in compression-tension would reveal greater stiffness degradation induced in the 0 degree plies at the surface than in the $\pm 45^\circ$ and 90° plies. In tension-tension mode, the inner plies would be more affected, while the overall stiffness degradation remains similar for both fatigue modes.

Another reason could be traced back to internal material degradation between the plies, which affects the stiffness parameters different from the Young's modulus in load direction. For example, the formation of delaminations at cross points of cracks between a 0° and a 45° layer leads to a decrease in the out-of-plane Young's modulus which is more pronounced if a compressive load is present. However, the overall stiffness degradation measured in load direction stays the same because delaminations and cracks parallel to the loading direction virtually do not affect the stiffness.

Conclusions

A methodology for non-destructive evaluation of fatigue caused by mechanical loads in plate-like NCF composite components has been proposed. A simple and inexpensive setup, based

on a single-sided access configuration of ACU, has been applied to remote monitoring stiffness degradation in composites by measuring variation in flexural wave velocity. The change in the velocity is found to be different for the tension-tension and compression-tension fatigue modes. Internal degradation caused by cyclic loading has been detected by an increase in attenuation of the flexural wave due to scattering on cracks. More experimental data is desirable for evaluations whether the combination of both velocity and attenuation is a distinctive parameter to distinguish different loading protocols. Based on the preliminary results obtained, depth-resolved monitoring of stiffness degradation due to fatigue is feasible by using plate ultrasonic waves. This could contribute to a better understanding of the manner composites degrade and fail due to different types of cyclic loads.

Acknowledgements

The authors are grateful to the German Research Foundation (DFG) for supporting this work as part of the project Bu 624/28-1 and Schu 926/16-1.

References

1. J. J. Nevadunsky, J. J. Lucas, M. J. Salkind: *Early Fatigue Damage in Composite Materials*, Journal of Composite Materials, v. 9, 394, 1975
2. T. K. O'Brien, K. L. Reifsnider: *Fatigue damage evaluation through stiffness measurements in boron-epoxy laminates*, Journal of Composite Materials, v. 15, 55–70, 1981
3. R. D. Jamison, K. Schulte, K. L. Reifsnider, W. W. Stinchcomb: *Characterization and Analysis of Damage Mechanisms in Tension-Tension Fatigue of Graphite/Epoxy Laminates*, Effects of Defects in Composite Materials, ASTM STP 836. American Society for Testing and Materials, pp. 21-55, 1984
4. W. Hufenbach, T. Ritzel, R. Böhm, A. Langkamp: *Ultrasonic Determination of Anisotropic Damage in Fibre and Textile Reinforced Composite Materials*, Conference on Damage in Composite Materials 2006, Stuttgart, Online-Proceedings
5. M. Rojek, J. Stabik, S. Sokól: *Fatigue and ultrasonic testing of epoxy-glass composites*, Journal of Achievements in Materials and Manufacturing Engineering, v. 20, Issues 1-2, January-February 2007
6. K. Mal, M. R. Gorman, and W. H. Prosser, *Material characterization of composite laminates using low-frequency plate wave dispersion data*, Review of Progress in Quantitative Nondestructive Evaluation 11, 1451-1458, 1992
7. W. H. Prosser, M. R. Gorman: *Plate mode velocities in graphite/epoxy plates*, Journal of the Acoustic Society of America 96, pp. 902-907, 1994
8. B. Tang, E. G. Henneke: *Lamb-Wave Monitoring of Axial Stiffness Reduction of Laminated Composite Plates*, Material Evaluation, v. 47, no. 8, pp. 928-934, 1989
9. M. D. Seale, B. T. Smith, and W. H. Prosser, *Lamb wave assessment of fatigue and thermal damage in composites*, Journal of the Acoustic Society of America 103, pp. 2416–2424, 1998
10. J.-H. Shih, A. K. Mal, and M. Vemuri: *Plate wave characterization of stiffness degradation in composites during fatigue*, Research in Nondestructive Evaluation. 10, 147–162, 1998
11. S. Adden, K. Pfleiderer, I. Solodov, P. Horst, G. Busse: *Characterization of Stiffness degradation caused by fatigue damage in textile composites using circumferential plate acoustic waves*, Composite Science and Technology, v. 68, pp. 1616-1623, 2008

12. A. J. Rogovsky: *Development and application of ultrasonic dry-contact and air-contact C-scan systems for non-destructive evaluation of aerospace components*, *material Evaluation*, 50, 1491-1497, 1991
13. M. Castaings, P. Cawley, R. Farlow, G. Hayward: *Single Sided Inspection of Composite Materials Using Air Coupled Ultrasound*, *Journal of Nondestructive Evaluation*, v. 17, No. 1, 1998
14. M. Castaings, B. Hosten: *Ultrasonic guided waves for health monitoring of high-pressure composite tanks*, *NDT&E International*, v. 41, pp. 648-655, 2008
15. I. A. Victorov: *Rayleigh and Lamb Waves*, Plenum Press, New York, 1967
16. I. Solodov, K. Pfeleiderer, G. Busse: *Laser vibrometry of air-coupled Lamb waves: a novel methodology for noncontact material characterization*, *Materialprüfung*, 47, 3, pp. 3-7. 2005
17. D. Döring, I. Solodov, and G. Busse: *Air-Coupled Surface Acoustic Waves: Opportunities and Limitations for NDT Application*, *Proc. 4th Workshop NDT in Progress*, Prague, 2007, pp. 51 – 62.
18. C.C. Habberger, R.W. Mann, G.A. Baum: *Ultrasonic plate waves in paper*, *Ultrasonics*, March 1979, pp. 57-62.